COBEM 2023 27TH INTERNATIONAL CONGRESS OF MECHANICAL ENGINEERING

ABCM Brazilian Society of Mechanical Sciences and Engineering
27th ABCM International Congress of Mechanical Engineering
December 04-08, 2023, Florianópolis-SC, Brazil

COB-2023-1342
PERFORMANCE ANALYSIS OF THERMOELECTRIC COOLERS IN SERIES AND PARALLEL CONFIGURATIONS

Bernardo P. Vieira
Jaime A. Lozano
Jader R. Barbosa Jr.
POLO — Research Laboratories for Emerging Technologies in Cooling and Thermophysics, Department of Mechanical Engineering, Federal University of Santa Catarina, Florianópolis, SC, 88040-900, Brazil
bernardo.vieira@polo.ufsc.br, jaime@polo.ufsc.br, jrb@polo.ufsc.br

Abstract. *Thermoelectric cooling is an alternative cooling technology with several desirable attributes, such as low weight, compactness and absence of a working fluid. It, however, has several limitations regarding performance, energy consumption and achievable temperature span. Because of this, several solutions have been proposed to try and improve the performance of this technology and make it more competitive in cooling applications. Among these solutions, some studies have proposed arranging the modules in series in order to achieve higher temperature spans and higher cooling capacities. In this work, a mathematical model was developed to simulate the operation of the modules in this configuration and compare it with the performance of the same number of modules operating independently (stacked). The results showed that the parallel configuration had a better performance than the series configuration, with the difference increasing with the number of modules. Meanwhile, the main advantage of the series configuration is its lower complexity. The parallel configuration, however, may be more affected by the fan losses, with further studies being needed to better quantify this effect on the performance.*

Keywords: *Peltier module, Thermoelectric cooling, Alternative cooling technologies*

1. INTRODUCTION

Thermoelectric cooling is an alternative cooling technology that consists of using Peltier modules which convert electrical energy (current or voltage) into cooling power through the Peltier effect. This technology has several desirable attributes, such as high reliability, no mechanical moving parts, low weight, compactness and absence of a working fluid. It also has the ability to be powered by direct current electric sources, allowing it to be integrated with renewable energy sources such as photovoltaic cells and fuel cells. This technology, however, has a high cost and low energy efficiency, restricting it application to systems where these parameters are less important than reliability and environmental impact (Zhao and Tan, 2014). Another characteristic of thermoelectric coolers (TECs) is the considerable reduction in efficiency they present when the temperature span is increased (Lee, 2017). One common way to allow for the modules to reach higher temperature spans is to organize them into vertical cascade arrangements (Karimi *et al.*, 2011). In these arrangements, the internal losses increase with the number of stages, and thus several solutions have been proposed to try and mitigate this effect in a wide range of applications, such as electronics cooling (Cai *et al.*, 2017) and thermal comfort (Rincón-Casado *et al.*, 2018).

Another way to arrange the models and obtain larger temperature spans is in series, with counter-current flow (Bell, 2008). This configuration allows the temperature span to be built up along the flows, making so that any given module is submitted to a smaller temperature span than the one between the outlets of each flow. This creates the potential to increase the COP of the system for a given temperature span (Provensi and Barbosa, 2020). While this configuration is promising, the contribution of each module to the performance continuously decreases the more modules are added to the system. Therefore, depending on the conditions, it may be more beneficial to have some modules operating independently instead of in series. To assess this, in this work, two module configurations will be analysed: in (i) series and in (ii) parallel (stacked). The series configuration consists of several modules organized side by side, with their hot and cold sides submitted to counter-current flows that build up the temperature increase on the hot side and decrease on the cold side. This configuration always has 2 fans regardless of the number of modules. The parallel or stacked configuration consists of each module operating independently with their own counter-current flow system. In this case, since each module is independent, the cooling capacity of N modules is simply N times the cooling capacity of a single module, but every new module adds another 2 fans to the system.

To compare these configurations, a numerical model was developed to solve both the internal operation of the modules and the heat exchange with the air flows. This model was used to analyse the performance of four commercially available modules with different operation ranges under different conditions and configurations. They were initially analysed

considering a system without external irreversibilities, i.e., with ideal heat exchange, in order to directly compare their performances without external disturbances. Next, the heat exchange model was activated and the effect of the flow velocity on the performance was analysed, highlighting the differences between low and high capacity modules in regards to required fluid flow rate. Lastly, the two previously mentioned configurations were compared in terms of cooling capacity and COP, with the results showing a considerable advantage of the stacked configuration over the series configuration.

2. MATHEMATICAL MODEL

2.1 Peltier Module

A thermoelectric module is comprised of a number of thermocouples (n), each one consisting of a p-type and an n-type semiconductor element, connected electrically in series and thermally in parallel. These are sandwiched between two ceramic plates which have low electrical conductivity but high thermal conductivity, allowing heat to flow through them, but preventing the passage of electrical currents. The modeling of these structures assumes that each thermocouple in a module operates independently, focusing on a single thermocouple and assuming that all others operate the same way. A schematic representation of a thermocouple with the relevant variables is shown in Figure 1.

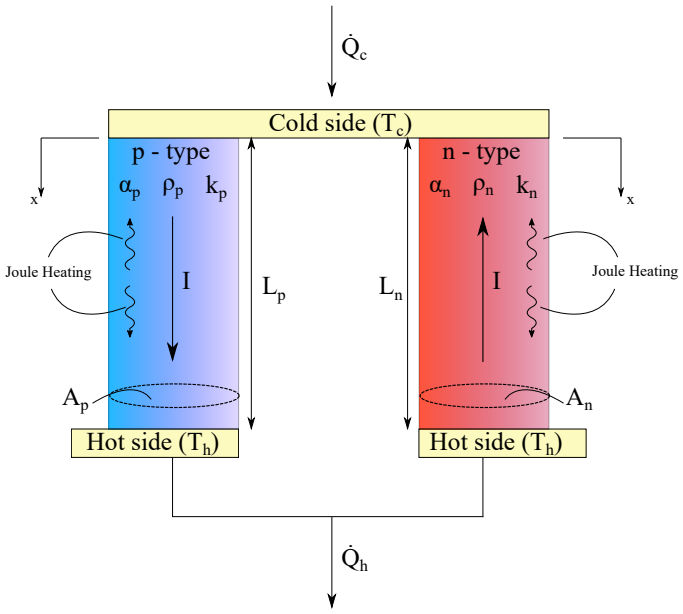

Figure 1. Schematic representation of a thermocouple within a module. Adapted from Lee (2017).

The general heat diffusion equation, which will be applied to the thermocouple, is given by:

$$-\vec{\nabla}.\vec{q} + \dot{q} = \frac{c}{v}\frac{\partial T}{\partial t} \tag{1}$$

where the first term represents the heat flux, the second term the heat generation and the third term the heat capacity of the material. c is the specific heat and v the specific volume. From the Thomson relationship and the Onsager's principle it is possible to show that:

$$\vec{q} = \alpha T\vec{j} - k\vec{\nabla}T \tag{2}$$

where α is the Seebeck coefficient and $\vec{j}$ is the current density. Furthermore, it can also be shown that (Lee, 2017):

$$\dot{q} = j^2\rho + \vec{j}.\alpha\vec{\nabla}T \tag{3}$$

where ρ is the electrical resistivity. Substituting Eqs. (2) and (3) into Eq. (1) and applying the continuity equation for a constant current ($\vec{\nabla}.\vec{j} = 0$) gives:

$$\vec{\nabla}.(k\vec{\nabla}T) + j^2\rho - T\frac{d\alpha}{dT}\vec{j}.\vec{\nabla}T = \frac{c}{v}\frac{\partial T}{\partial t} \tag{4}$$

where the first term is the thermal conduction, the second term is the Joule heating, the third term is the Thomson heat and the fourth term is the heat capacity. To simplify the solution, the following assumptions can be made (Lee, 2017):

- Steady-state;
- One-dimensional conduction;
- Negligible thermal and contact resistances;
- Negligible convection and radiation at the surfaces;
- Constant properties.

Reducing Eq. (4) to:

$$\frac{d}{dx}\left(kA\frac{dT}{dx}\right) + \frac{I^2\rho}{A} = 0 \tag{5}$$

where I is the electrical current. This is an equation that can be solved analytically. After an appropriate integration with boundary conditions $T_{\mathrm{x=0}} = T_{\mathrm{c}}$ and $T_{\mathrm{x=L}} = T_{\mathrm{h}}$, the resulting equations can be evaluated at $x = 0$ to determine the cooling capacity ($\dot{Q}_{\mathrm{c}}$) of n thermocouples:

$$\dot{Q}_{\mathrm{c}} = n\left[\alpha T_{\mathrm{c}} I - \frac{1}{2}I^2R - K(T_{\mathrm{h}} - T_{\mathrm{c}})\right] \tag{6}$$

where:

$$\alpha = \alpha_{\mathrm{p}} - \alpha_{\mathrm{n}} \quad , \quad R = \frac{\rho_{\mathrm{p}}L_{\mathrm{p}}}{A_{\mathrm{p}}} + \frac{\rho_{\mathrm{n}}L_{\mathrm{n}}}{A_{\mathrm{n}}} \quad , \quad K = \frac{k_{\mathrm{p}}A_{\mathrm{p}}}{L_{\mathrm{p}}} + \frac{k_{\mathrm{n}}A_{\mathrm{n}}}{L_{\mathrm{n}}} \tag{7}$$

Equation (6) is known as the *ideal equation* and is widely used in research and modeling involving thermoelectric cooling. Note that the first term represents the Peltier effect, responsible for the cooling, while the second term represents the Joule heating and the third term the thermal conduction along the semiconductor, both of which reduce the cooling capacity. A similar approach can be applied to $x = L$ to determine the rate of heat rejection, giving:

$$\dot{Q}_{\mathrm{h}} = n\left[\alpha T_{\mathrm{h}} I + \frac{1}{2}I^2R - K(T_{\mathrm{h}} - T_{\mathrm{c}})\right] \tag{8}$$

Note that, in this case, the Joule heating increases the rejected heat, as would be expected.

The first law of thermodynamics gives that the total electrical work input can be calculated from the difference between $\dot{Q}_{\mathrm{h}}$ and $\dot{Q}_{\mathrm{c}}$, resulting in:

$$\dot{W}_{\mathrm{e}} = \dot{Q}_{\mathrm{h}} - \dot{Q}_{\mathrm{c}} = n[\alpha I(T_{\mathrm{h}} - T_{\mathrm{c}}) + I^2R] \tag{9}$$

where the first term on the right is the rate of work required to overcome the thermoelectric voltage and the second term is the resistive loss. Since the power is $\dot{W}_{\mathrm{e}} = VI$, the voltage across the thermocouple will be:

$$V = n[\alpha(T_{\mathrm{h}} - T_{\mathrm{c}}) + IR] \tag{10}$$

Finally, the Coefficient of Performance (COP), defined as the ratio between the cooling power and the electrical work input is given by:

$$\mathrm{COP} = \frac{\dot{Q}_{\mathrm{c}}}{\dot{W}_{\mathrm{e}}} = \frac{\alpha T_{\mathrm{c}} I - \frac{1}{2}I^2R - K(T_{\mathrm{h}} - T_{\mathrm{c}})}{\alpha I(T_{\mathrm{h}} - T_{\mathrm{c}}) + I^2R} \tag{11}$$

which is a function only of the module's properties, the electric current and the temperature span.

2.2 Module with Heat Exchange Fluid

In most real thermoelectric systems, the Peltier module does not exchange heat directly with the hot and cold sources, but instead indirectly through a heat exchange fluid (usually air or water). It is common for the heat exchange between the module and the fluid to be enhanced through the use of fins or other similar structures. Figure 2 shows a schematic representation of a module within a system with these characteristics. In this case, the heat exchange enhancer is represented by fins and the heat exchange fluid is air which flows through the use of fans, but these selections only affect the fluid properties and the closure relationships, not the thermal modeling that will be discussed in this section.

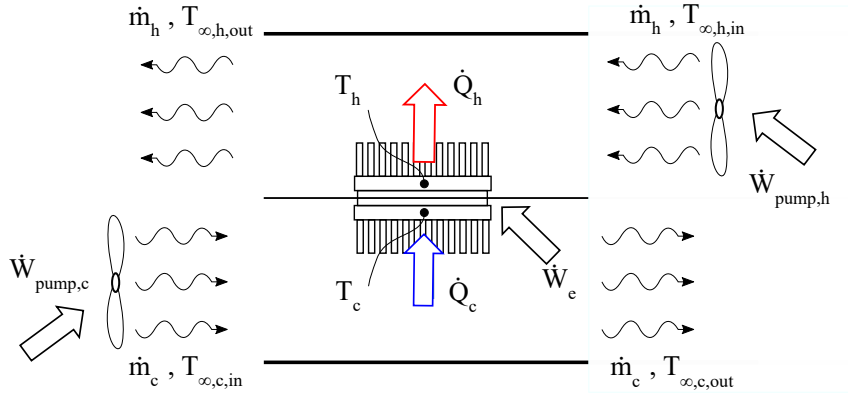

Figure 2. Schematic representation of a Peltier module within a system including fins and fans.

Note that if the current, the mass flow rates and the inlet temperatures are entry parameters, there are six unknown variables in Figure 2: $\dot{Q}_\mathrm{h}$, $\dot{Q}_\mathrm{c}$, T_h, T_c, $T_{\infty,\mathrm{h,out}}$ and $T_{\infty,\mathrm{c,out}}$. Thus, six equations are needed to solve the mathematical system. The first two are Eqs. (6) and (8) from the last section, which give the cooling capacity and heat exchange from the module's theory. The next two are obtained from the convection heat transfer between the module and the fluid, resulting in:

$$\dot{Q}_\mathrm{c} = \frac{\overline{T}_{\infty,\mathrm{c}} - T_\mathrm{c}}{R_{\mathrm{th,c}}} \quad , \quad \dot{Q}_\mathrm{h} = \frac{T_\mathrm{h} - \overline{T}_{\infty,\mathrm{h}}}{R_{\mathrm{th,h}}} \tag{12}$$

where $\overline{T}_{\infty,\mathrm{c}}$ and $\overline{T}_{\infty,\mathrm{h}}$ are the average temperatures between the inlet and outlet in the cold and hot sides, respectively, and $R_{\mathrm{th,c}}$ and $R_{\mathrm{th,h}}$ are the cold and hot side's combined thermal resistances between the module and the air flow. These resistances are obtained through closure relationships that depend, among other things, on the fluid, the type of flow and the heat exchange enhancer. In this work, the fluid was assumed to be air and the heat exchange enhancer was an array of fins, with the thermal resistance being determined using the model developed by Khan and Yovanovich (2007) and Khan *et al.* (2008). The last two equations come from the energy balance on the air flow assuming (i) steady state, (ii) no shaft or boundary work, (iii) negligible changes in kinetic and potential energy and (iv) thermally insulated channel walls:

$$\dot{Q}_\mathrm{c} = \dot{m}_\mathrm{c} c_{\mathrm{p,c}} (T_{\infty,\mathrm{c,in}} - T_{\infty,\mathrm{c,out}}) \quad , \quad \dot{Q}_\mathrm{h} = \dot{m}_\mathrm{h} c_{\mathrm{p,h}} (T_{\infty,\mathrm{h,out}} - T_{\infty,\mathrm{h,in}}) \tag{13}$$

where c_p is the fluid's specific heat capacity at a constant pressure. This adds up to six equations for six unknowns, and allows for the model to be solved if given the proper closure relationships for the thermal resistances. The electrical work in this case can still be calculated using Eq. (9), but the pumping power also needs to be considered to evaluate the system's performance, and it is given by:

$$\dot{W}_\mathrm{p} = \dot{W}_{\mathrm{p,c}} + \dot{W}_{\mathrm{p,h}} = \dot{m}_\mathrm{c} v_\mathrm{c} \Delta P_\mathrm{c} + \dot{m}_\mathrm{h} v_\mathrm{h} \Delta P_\mathrm{h} \tag{14}$$

where ΔP is the pressure drop in the channel, given by the closure relationships modeling the heat exchange enhancer. Lastly, the COP is then calculated as:

$$\mathrm{COP} = \frac{\dot{Q}_\mathrm{c}}{\dot{W}_\mathrm{e} + \dot{W}_\mathrm{p}} \tag{15}$$

However, it is possible to arrange several modules one after the other in order to reach higher cooling powers (Provensi and Barbosa, 2020), resulting in a system like the one shown in Figure 3. In this case, the six equations need to be solved for each module, resulting in a system with the following equations:

$$\begin{cases} \dot{Q}_{\mathrm{c,j}} = n_{\mathrm{j}}\left[\alpha_{\mathrm{j}} T_{\mathrm{c,j}} I_{\mathrm{j}} - \dfrac{1}{2} I_{\mathrm{j}}^2 R_{\mathrm{j}} - K_{\mathrm{j}}(T_{\mathrm{h,j}} - T_{\mathrm{c,j}})\right] \\ \dot{Q}_{\mathrm{h,j}} = n_{\mathrm{j}}\left[\alpha_{\mathrm{j}} T_{\mathrm{h,j}} I_{\mathrm{j}} + \dfrac{1}{2} I_{\mathrm{j}}^2 R_{\mathrm{j}} - K_{\mathrm{j}}(T_{\mathrm{h,j}} - T_{\mathrm{c,j}})\right] \\ \dot{Q}_{\mathrm{c,j}} = \dfrac{\overline{T}_{\infty,\mathrm{c,j}} - T_{\mathrm{c,j}}}{R_{\mathrm{th,c,j}}} \\ \dot{Q}_{\mathrm{h,j}} = \dfrac{T_{\mathrm{h,j}} - \overline{T}_{\infty,\mathrm{h,j}}}{R_{\mathrm{th,c,j}}} \\ \dot{Q}_{\mathrm{c,j}} = \dot{m} c_{\mathrm{p,j}} (T_{\infty,\mathrm{c,j}} - T_{\infty,\mathrm{c,j+1}}) \\ \dot{Q}_{\mathrm{h,j}} = \dot{m} c_{\mathrm{p,j}} (T_{\infty,\mathrm{h,j}} - T_{\infty,\mathrm{h,j+1}}) \end{cases} \tag{16}$$

where $0 < j < N-1$ with N being the number of modules. Note that, in this case, the total cooling capacity, rejected heat, electrical work input and pumping power will be the sum of the contributions of each individual module, being given by:

$$\dot{Q}_{\mathrm{c,total}} = \sum_{j=0}^{N-1} \dot{Q}_{\mathrm{c,j}} \quad , \quad \dot{Q}_{\mathrm{h,total}} = \sum_{j=0}^{N-1} \dot{Q}_{\mathrm{h,j}} \quad , \quad \dot{W}_{\mathrm{e,total}} = \sum_{j=0}^{N-1} \dot{W}_{\mathrm{e,j}} \quad , \quad \dot{W}_{\mathrm{p,total}} = \sum_{j=0}^{N-1} \dot{W}_{\mathrm{p,c,j}} + \sum_{j=0}^{N-1} \dot{W}_{\mathrm{p,h,j}} \tag{17}$$

and the COP of the system will be:

$$\mathrm{COP} = \frac{\dot{Q}_{\mathrm{c,total}}}{\dot{W}_{\mathrm{e,total}} + \dot{W}_{\mathrm{p,total}}} \tag{18}$$

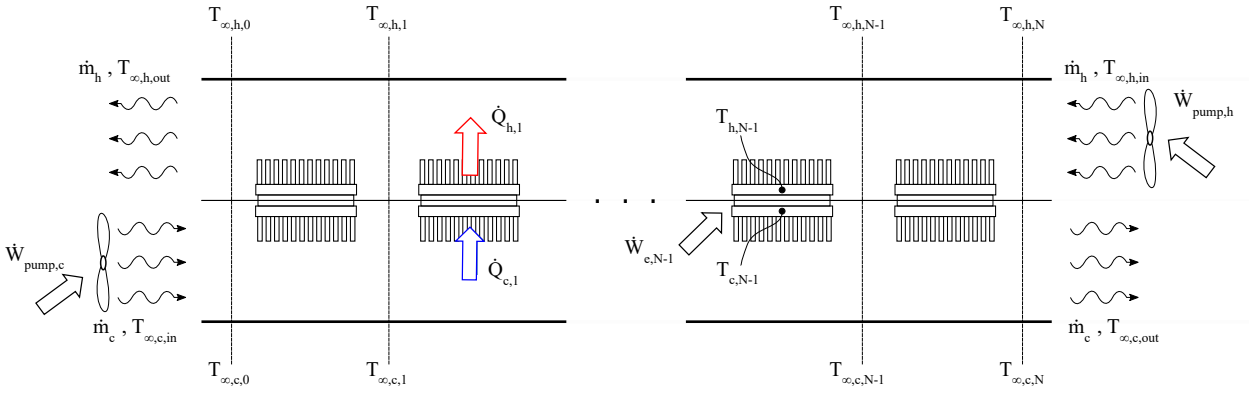

Figure 3. Schematic representation of several Peltier modules within the system including fins and fans.

3. RESULTS AND DISCUSSION

3.1 Test Modules

In this work, four commercially available Peltier modules with different characteristics, described in Table 1, were selected for testing. They were chosen with the goal of contemplating different classes of available modules, with Module 1 representing low cooling capacity, lower cost modules, Module 4 representing high cooling capacity, higher cost modules, and Modules 2 and 3 representing intermediate modules.

Table 1. Characteristics of the commercial Peltier modules used in this study. All modules are square-shaped with width and length of 40 mm.

#	N_e	A_e [mm²]	L_e [mm]	I_{max} [A]	$\dot{Q}_{max}$ [W]	ΔT_{max} [K]	t_m [mm]
1	127	1.96	2.5	3.8	38	74	4.8
2	127	1.96	1.15	8.0	80	71	3.4
3	199	1.96	1.05	8.6	131	69	3.5
4	199	1.96	0.6	15.1	229	68	3.1

3.2 Performance with Ideal Heat Exchange

Initially, the modules will be analyzed assuming an ideal heat exchange, i.e., without a thermal resistance between the module and the heat exchange fluid, reducing the problem to simply solving the equations presented in Section 2.1 . In other words, the system is assumed internally irreversible, but externally reversible. This analysis allows not only for an initial comparison of the modules, but also gives a ceiling for the performance of each module, since any real heat exchanging structure will have a thermal resistance that will add irreversibilities to the system.

Figure 4 shows the results for cooling capacity of all four modules as a function of the electric current for a fixed hot side temperature (35 ºC) and two different cold side temperatures: 25 ºC and 5 ºC. Note that all modules are affected by the reduction of T_c the same way: the cooling power is reduced and the current at which the maximum cooling power happens decreases. In relation to each other, it is clear that Module 4 is able to reach higher values of $\dot{Q}_c$ than any other module by a considerable margin, followed by Modules 3, 2 and 1. On the other hand, Figure 5 shows the COP of all modules for the same conditions. Note that in both cases Module 1 is able to reach the highest COP, followed by Modules 2 and 3, which are very similar, and then Module 4. This trade-off between cooling power and COP is rather common for commercially available modules and must be taken into account when selecting the appropriate one for a thermoelectric cooling system.

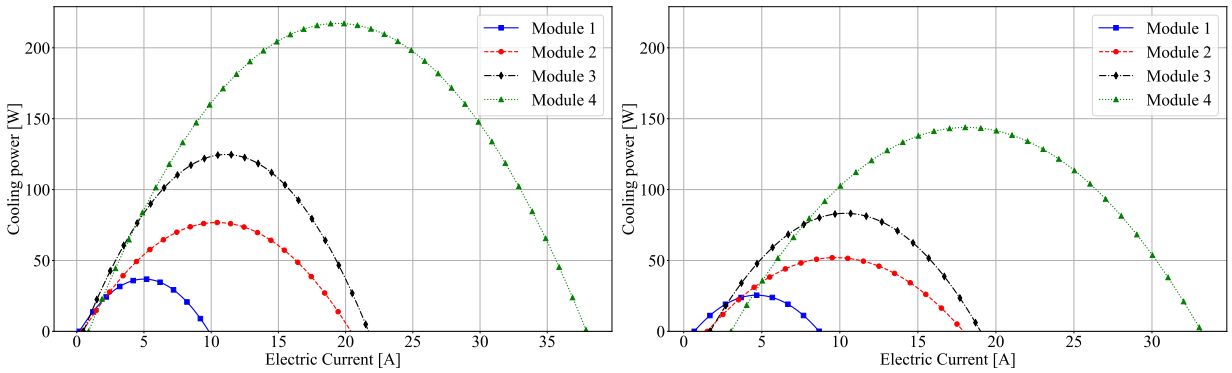

Figure 4. Cooling power as a function of the electric current for each module with a T_h of 35 ºC and a T_c of (a) 25 ºC and (b) 5 ºC.

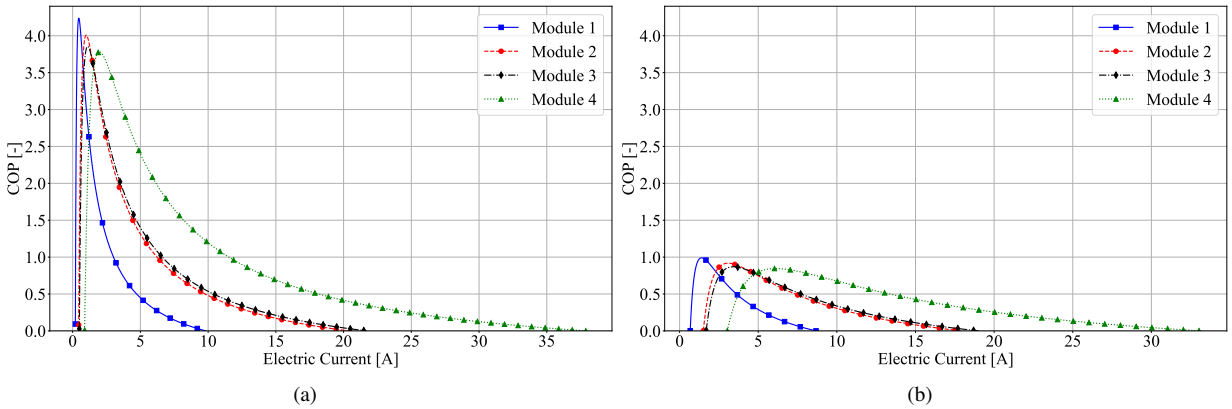

Figure 5. COP as a function of the electric current for each module with a T_h of 35 ºC and a T_c of (a) 25 ºC and (b) 5 ºC.

Table 2 summarizes the results shown in Figures 4 and 5 by listing the maximum values of $\dot{Q}_c$ and COP for each

case and also for cold side temperatures of 15 ºC and -5 ºC. As discussed above, these values are the highest that may possibly be achieved by each module for each temperature span, since they only consider the irreversibilities inherent to the modules themselves and none from the rest of the system. Therefore, the design of the system should aim to get as close as possible to these values, as surpassing them would be impossible without improving the modules themselves.

Table 2. Maximum values of $\dot{Q}_c$ and COP for all modules operating with ideal heat exchange and a hot side temperature of 35 ºC and different cold side temperatures, T_c.

	T_c							
	25 °C		15 °C		5 °C		-5 °C	
#	$\dot{Q}_{c,max}$ [W]	**COP** [-]	$\dot{Q}_{c,max}$ [W]	**COP** [-]	$\dot{Q}_{c,max}$ [W]	**COP** [-]	$\dot{Q}_{c,max}$ [W]	**COP** [-]
1	36.86	4.24	31.12	1.80	25.47	0.99	19.91	0.58
2	76.75	4.01	64.27	1.69	51.99	0.92	39.89	0.53
3	124.73	3.86	103.84	1.61	83.25	0.87	62.96	0.50
4	217.20	3.78	180.24	1.58	143.83	0.84	107.94	0.48

3.3 Performance with Fin Arrays and Ideal Fans

In this section, the heat exchange between each side of the Peltier module and the fluid will no longer be considered ideal, but instead happen through a 15 by 15 fin array of staggered cylindrical fins, with a diameter of 2 mm and height of 30 mm. The air flow will be provided by an ideal fan, i.e, with no losses and capable of operating in any desired pressure drop x flow rate condition. In this analysis, the duct has a height of 48.6 mm and a width of 60 mm, which is enough to house the module with the fins. These dimensions were chosen because they presented a good relation between heat exchange and pressure drop. This configuration adds a new variable that influences the system performance: the mass flow rate of the fluid. Because the effects of the viscous dissipation is not considered in the modeling, the influence of the mass flow rate is fairly straightforward: if increased, it improves the heat exchange (higher heat transfer coefficient), but also increases the pumping power of the system.

This can be seen in Figures 6 and 7, which respectively show the cooling power and the COP of modules 1 and 4 for different mass flow rates. Note that, for the cooling power, increasing the mass flow rate is strictly positive, and brings the cooling power profile increasingly closer to the ideal one shown in Figure 4, since $h \to \infty$ as $\dot{m} \to \infty$. This has a positive effect on the COP, however, as seen in the COP results for Module 1, at a certain point, the detriment caused by the increase in pumping power due to both the increase in pressure drop and the mass flow rate itself (see Eq. (14)) surpasses the benefit of increasing the cooling power, and the COP starts to decrease. It should also be noted that the higher the cooling power the module is able to achieve, the more it favors higher mass flow rates, not only by requiring higher values to maximize the cooling power and the COP, but also by performing considerably worse than the other modules at low mass flow rates.

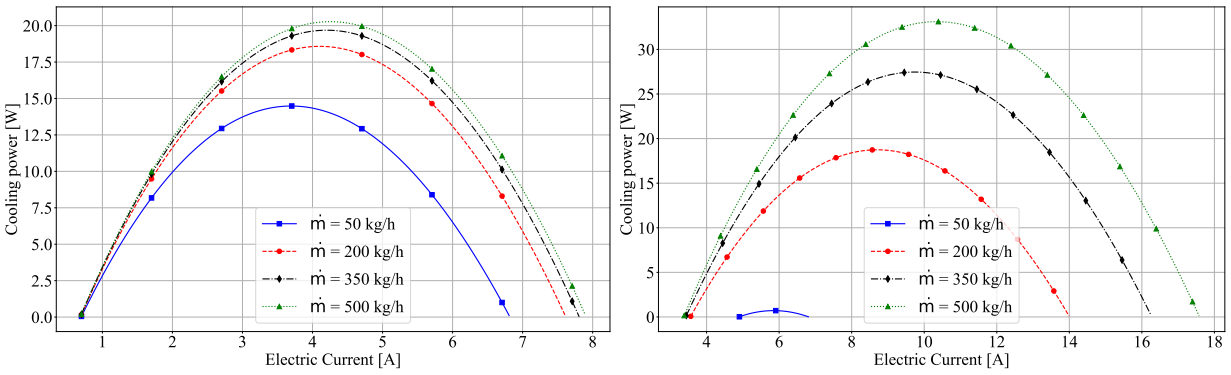

Figure 6. Cooling power of Modules (a) 1, and (b) 4 as a function of the electric current for different mass flow rates. T_h was set to 35 ºC and T_c to 5 ºC.

All these conclusions become even more apparent in Figure 8, that shows the maximum cooling power and COP for each module as a function of the mass flow rate. Analysing the first plot, it can be seen that after a certain value of mass flow rate the increase in cooling power slows considerably, and increasing the mass flow rate becomes less interesting for the performance. The value at which this happens goes from around 100 kg/h for Module 1 to over 800 kg/h for Module 4. Another interesting result is that, for almost all mass flow rates shown, Module 3 has a better performance in both cooling power and COP than Module 4. This shows that module selection needs to go beyond just looking at the

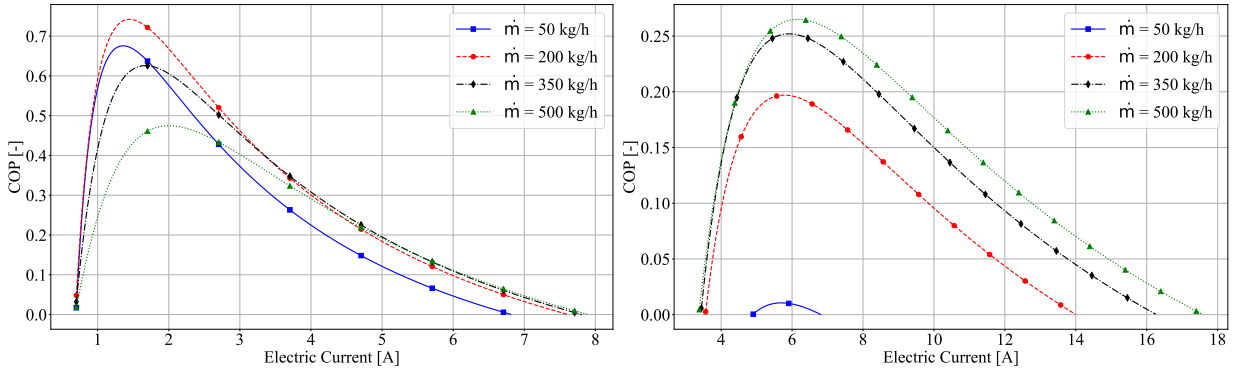

(a) (b)

Figure 7. COP of Modules (a) 1 and (b) 4 as a function of the electric current for different mass flow rates. T_{h} was set to 35 ºC and T_{c} to 5 ºC.

catalogue, because while one might expect Module 4 to reach higher cooling powers than Module 3, this is only true if a sufficiently high heat transfer coefficient can be reached by the system, which is not always the case. Regarding the COP, Module 1 is capable of reaching the highest value while Module 4 reaches the lowest, as seen in Section 3.2, with the former reaching the maximum COP at lower mass flow rates than the latter, due to the stagnation of the cooling power in Module 1 and continuous increase of the pumping power.

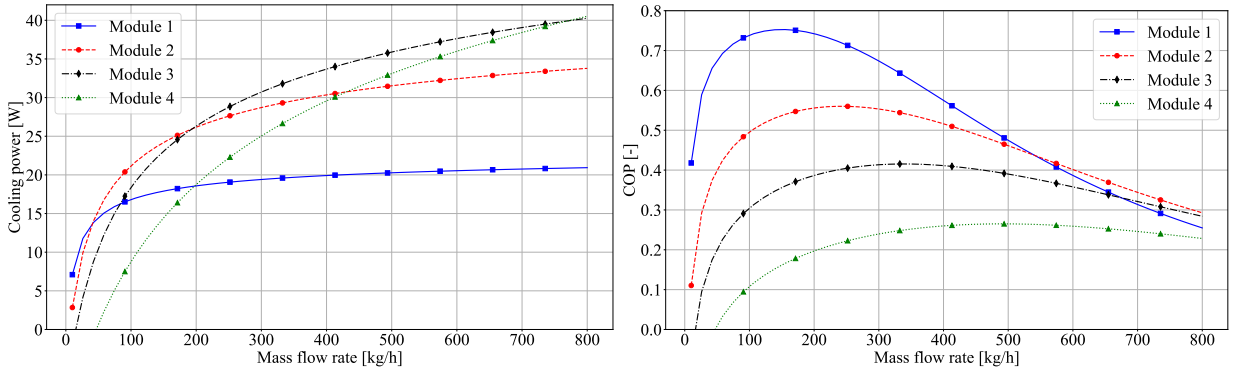

(a) (b)

Figure 8. Maximum (a) cooling power and (b) COP as a function of the mass flow rate for the four test modules.

In many cases, however, the cooling power obtained by a single module is not sufficient to meet the requirements of a refrigeration system and thus two or more modules have to be used. This gives rise to the question of how the modules should be arranged in order to optimize the performance. In this work, two possible arrangements will be analysed: (i) arranging the modules in series, like shown in Figure 3, and (ii) stacking several systems like the one shown in Figure 2, resulting in the configuration shown in Figure 9. The first configuration can be modeled using the method described in the previous section with N $>$ 1, while the second configuration can use the same modeling for a single module, and then multiply the main performance parameters (cooling power, rejected heat, work input) by N.

Since these systems are comprised of more than one module, each module may, in theory, operate under a different electrical current. However, in both cases it is better for all modules to operate under the same current. This is easy to see for the stacked case since each module operates independently and under the same conditions, and thus there is no reason for one to have an optimal current different from the other for a given application. For the series configuration this is less clear, since the performance of one module affects the next one. In fact, rigorously speaking, simulation results show that if the goal is optimizing cooling power, it is slightly better to operate the modules with continuously decreasing currents, however, this increase is very small (usually $<$ 1 %) and does not justify the increase in complexity required to operate under such conditions. Furthermore, the maximum COP was always reached when all modules operated under the same current.

An important difference between the stacked and the series configuration is the number of fans: while the first uses 2N, the second only uses two. Because of this, one might think that for a fair comparison the stacked configuration should operate with a mass flow rate that is N times smaller than the series configuration. However, since all the pressure drop is assumed to be caused by the heat exchange enhancers (fins), which all have the same pressure drop for a given mass flow rate, a configuration with N modules would have approximately the same pressure drop (and thus require the same

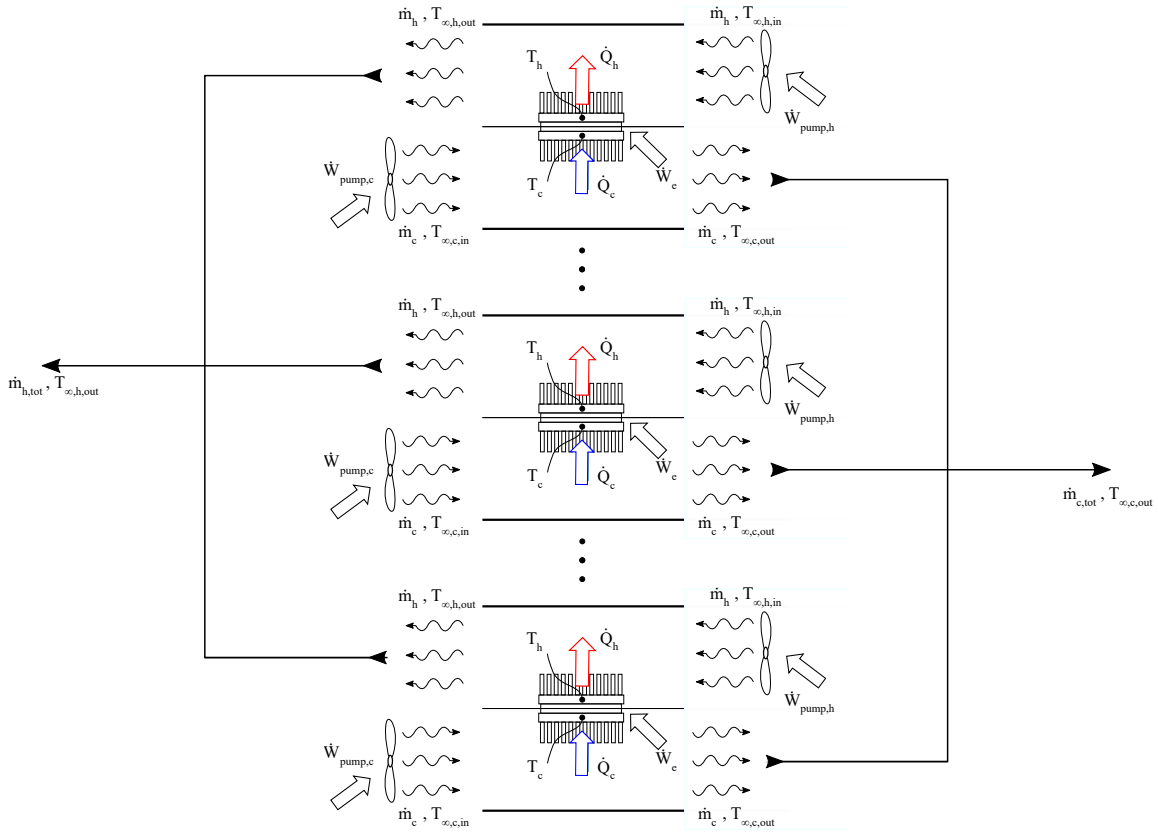

Figure 9. Schematic representation of the stacked Peltier modules configuration.

pumping power) regardless of its type (series or stacked), so long as the mass flow rate of each fan is the same in both cases. Therefore, in this section, both configurations were compared when operating under the same mass flow rate and thus the same pumping power.

This, however, gives an advantage to the stacked configuration because, while the mass flow rate in each module is the same between both cases, the total mass flow rate for the stacked configuration is N times larger than for the series configuration, and thus requires a smaller reduction of the fluid temperature to reach the same cooling power, reducing the temperature span to which the modules themselves are submitted and increasing their efficiency. This can be seen in Figure 10, that shows the maximum COP and cooling capacity obtained by each configuration as a function of the number of modules. As expected, the stacked configuration was strictly better than the series configuration, both in terms of cooling power and COP, with the difference between both growing as the number of modules increases. In fact, for the case in Figure 10, the stacked configuration had 30% more cooling capacity than the series configuration when 10 modules were used and 71% for 20 modules. Meanwhile, the COP of the stacked configuration remained constant at 0.74 while the COP of the series configuration dropped to 0.51 at 20 modules. Another way to visualize this is shown in Figure 11, which depicts the COP as a function of the cooling power for both configurations and different numbers of modules for Module 3. Note that for any given cooling power the stacked configuration is equal or superior to the series configuration regarding the COP, and that the series configuration is able to reach the same COP regardless of the number of modules. While only results for Modules 1 and 3 were shown, all modules had the same behaviour and the same conclusions can be drawn for them.

From the results, it can be concluded that, in general, the stacked configuration is superior in performance to the series configuration and should be chosen in all cases where the addition in complexity it brings can be overcome. However, it is important to highlight that all fans were considered ideal in this work, and their influence in both the work input and the heat dissipation into the refrigerated compartment may be relevant to the overall system performance, especially in the stacked case, which has a larger number of fans. However, since the series configuration will require a larger fan, the overall effect of the fans may be fairly similar between both cases resulting in similar conclusions to the ones obtained with ideal fans. In fact, with the considerations made in this model, it can be shown that if all fans have the same efficiency, the relation between the results of each configurations remains unchanged. However, some of the considerations that were made prevent the model from fully describing the behaviour of the flow and thus make it unable to precisely quantify the effects of the fans, with further works considering both real fan curves and a more detailed fluid flow model being needed to better describe the effects of the fans in the performance.

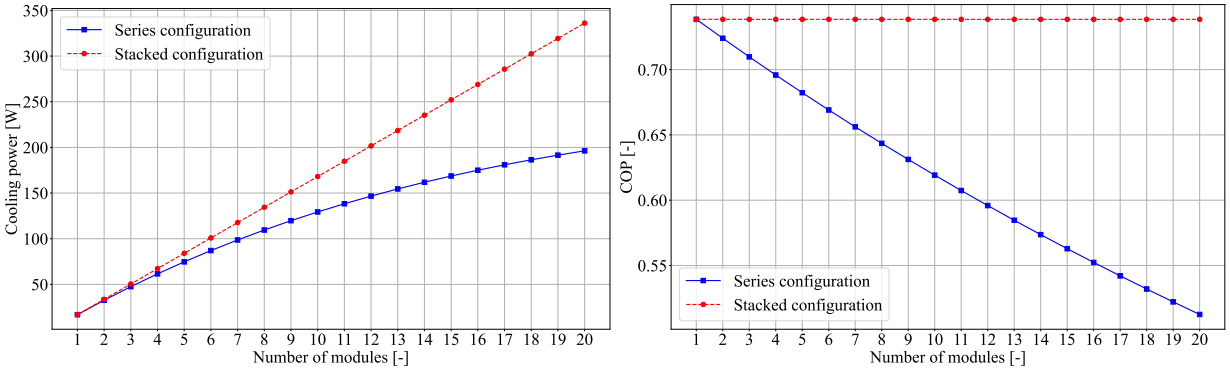

(a) (b)

Figure 10. Maximum (a) cooling power and (b) COP as a function of the number of modules. The results were obtained for Module 1, operating at a mass flow rate of 100 kg/h.

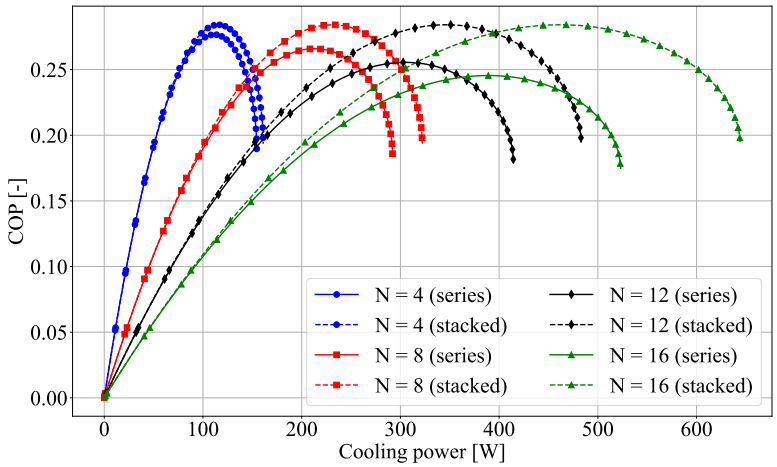

Figure 11. COP as a function of the cooling capacity for both configurations (series and stacked) and different numbers of modules. The results were obtained for Module 3, operating at a mass flow rate of 800 kg/h.

4. CONCLUSION

In this work, a mathematical model was developed to determine the performance of Peltier modules operating both in series and in parallel and then used to compare both scenarios. The internal model of the modules was developed using the general heat diffusion equation, the Thomson relationship and Onsager's principle, which resulted in an equation that was analytically solved by considering steady-state, one-dimensional conduction with negligible contact resistances and heat losses and constant properties. This resulted in analytical expressions for both the cooling capacity and rejected heat and, consequently, for the work input and the COP. The model was then enhanced to include heat exchange through the use of fin arrays, which was calculated using the model developed by Khan and Yovanovich (2007). The model was then used to determine the performance of 4 commercially available modules with different operating conditions. Initially, they were analysed considering ideal heat exchange in order to determine a baseline for comparison and to compare their performances without any external interferences. This was followed by an analysis of the effect of the mass flow rate on the performance with real heat exchange which showed that larger capacity modules require higher mass flow rates of air, and depending on the available mass flow rate, smaller modules may yield better performance than larger modules which are better on paper. Finally, the performance of the modules when arranged in series was compared with the performance of the same number of modules arranged in parallel (stacked configuration), and the results showed that, at the cost of a more complex system, the parallel configuration had better performance results, with the difference between the configurations increasing with the number of modules. This study, however, did not take into account the effect of the fan's irreversibilities, which may have a greater effect on the stacked modules than on the series configurations. Further studies considering real fans and with a more detailed modelling of the flow through the fins are needed to better quantify these effects.

Acknowledgements

The authors acknowledge the financial support from the Brazilian agencies CNPq, FAPESC and CAPES.

5. REFERENCES

Bell, L.E., 2008. "Cooling, heating, generating power, and recovering waste heat with thermoelectric systems". *Science*, Vol. 321, pp. 1457–1461.

Cai, Y., Liu, D., Yang, J.J., Wang, Y. and Zhao, F.Y., 2017. "Optimization of thermoelectric cooling system for application in cpu cooler". *Energy Procedia*, Vol. 105, pp. 1644–1650. ISSN 18766102. doi:10.1016/j.egypro.2017.03.535.

Karimi, G., Culham, J. and Kazerouni, V., 2011. "Performance analysis of multi-stage thermoelectric coolers". *International Journal of Refrigeration*, Vol. 34, pp. 2129–2135. ISSN 01407007. doi:10.1016/j.ijrefrig.2011.05.015.

Khan, W.A., Culham, J.R. and Yovanovich, M.M., 2008. "Optimization of pin-fin heat sinks in bypass flow using entropy generation minimization method". *Journal of Electronic Packaging*, Vol. 130. ISSN 1043-7398. doi: 10.1115/1.2965209.

Khan, W.A. and Yovanovich, M.M., 2007. "Effect of bypass on overall performance of pin-fin heat sinks". *Journal of Thermophysics and Heat Transfer*, Vol. 21, pp. 562–567. ISSN 0887-8722. doi:10.2514/1.27544.

Lee, H., 2017. *Thermoelectrics Desing and Materials*. Wiley, 1st edition.

Provensi, A. and Barbosa, J.R., 2020. "Analysis and optimization of air coolers using multiple-stage thermoelectric modules arranged in counter-current flow". *International Journal of Refrigeration*, Vol. 110, pp. 19–27. ISSN 01407007. doi:10.1016/j.ijrefrig.2019.10.014.

Rincón-Casado, A., Martinez, A., Araiz, M., Pavón-Domínguez, P. and Astrain, D., 2018. "An experimental and computational approach to thermoelectric-based conditioned mattresses". *Applied Thermal Engineering*, Vol. 135, pp. 472–482. ISSN 13594311. doi:10.1016/j.applthermaleng.2018.02.084.

Zhao, D. and Tan, G., 2014. "A review of thermoelectric cooling: Materials, modeling and applications". *Applied Thermal Engineering*, Vol. 66, pp. 15–24. ISSN 13594311. doi:10.1016/j.applthermaleng.2014.01.074.

6. RESPONSIBILITY NOTICE

The authors are solely responsible for the printed material included in this paper.